

Magnetic Signatures of the January 15 2022 Hunga Tonga–Hunga Ha`apai Volcanic Eruption

N. R. Schnepf¹, T. Minami², H. Toh³, and M. C. Nair^{4,5}

1- University of Colorado Boulder, Laboratory for Atmospheric and Space Physics, Boulder, 80305, USA

2- Kobe University, Department of Planetology, Kobe, 657-8501, Japan

3- Kyoto University, Data Analysis Centre for

Geomagnetism and Space Magnetism, Kyoto, 606-8502, Japan

4- University of Colorado Boulder, Cooperative Institute for Research in Environmental Sciences, Boulder, 80305, USA

5- National Oceanic and Atmospheric Administration, National Centers for Environmental Information, Boulder, 80305, USA

Contents of this file

Figures S1 to S26

Introduction

The figures here serve to complement those in the main paper. We provide more information on the locations of the Western Samoa, Honolulu, Easter Island, and Papeete observatories; raw data from each observatory; and the spectrograms resulting from the cross-wavelet analysis (for both a maximum period of 30 minutes and 120 minutes) of each observatory with the Alice Springs observatory.

Geomagnetic conditions

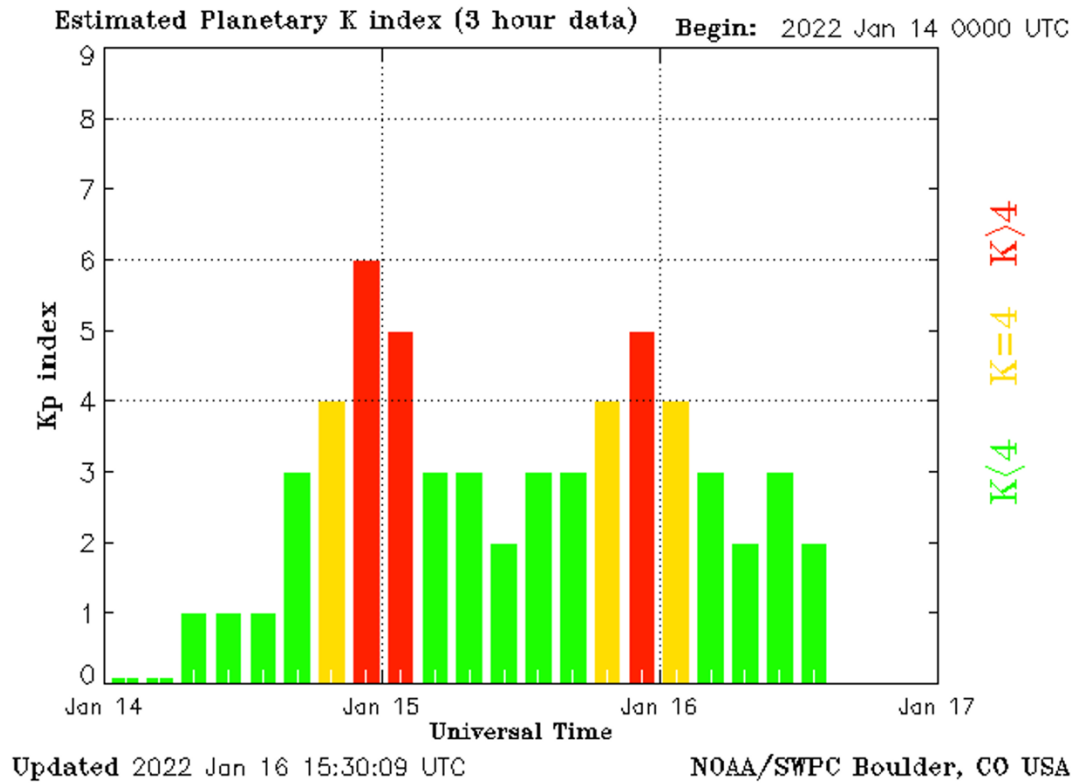


Figure S1. The Kp index on January 14-16, 2022 .

Detailed view of the observatory locations

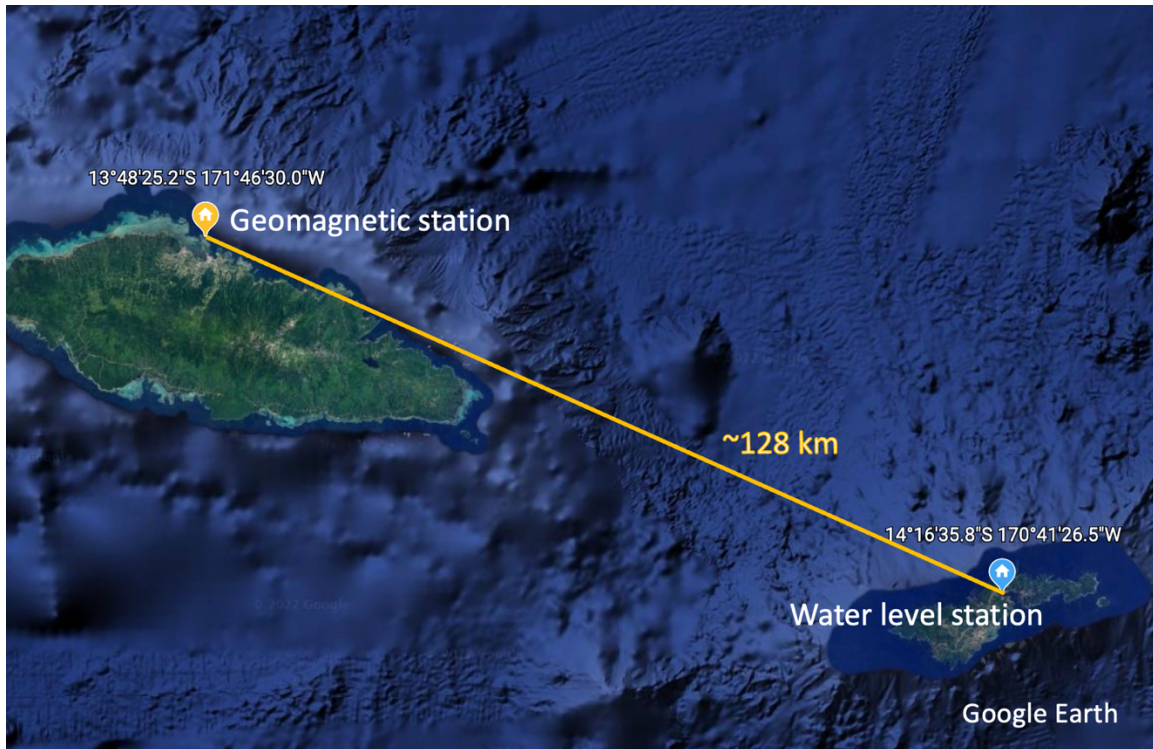


Figure S2. Location of the Western Samoa geomagnetic observatory relative to the water level station.



Figure S3. Location of the Honolulu, USA geomagnetic observatory relative to the coast.



Figure S4. Location of the Easter Island, Chile geomagnetic observatory relative to the coast.



Figure S5. Location of the Papeete, Tahiti, French Polynesia geomagnetic observatory relative to the coast.

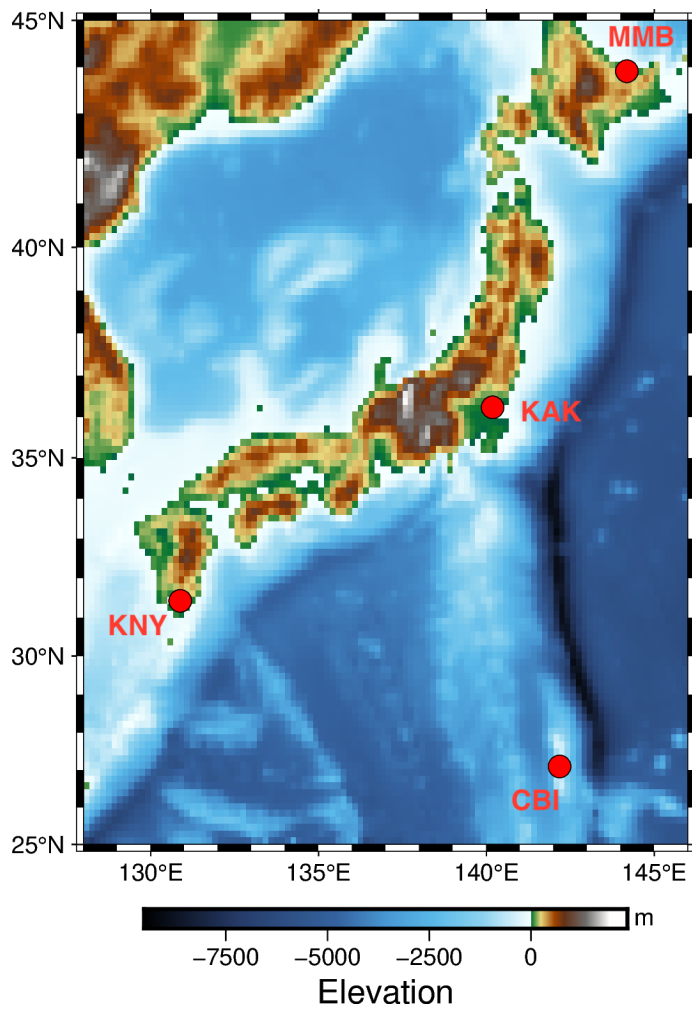


Figure S6. Map of the Japanese observatories.

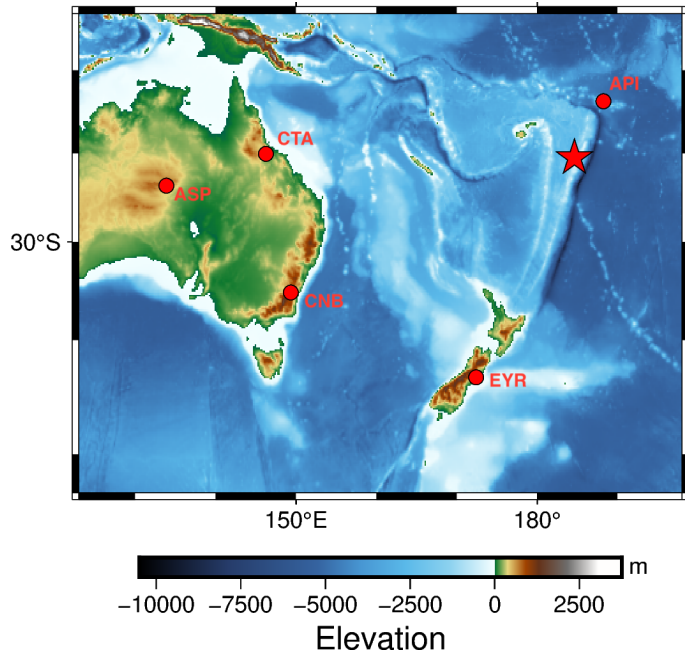


Figure S7. Map of the Oceania observatories.

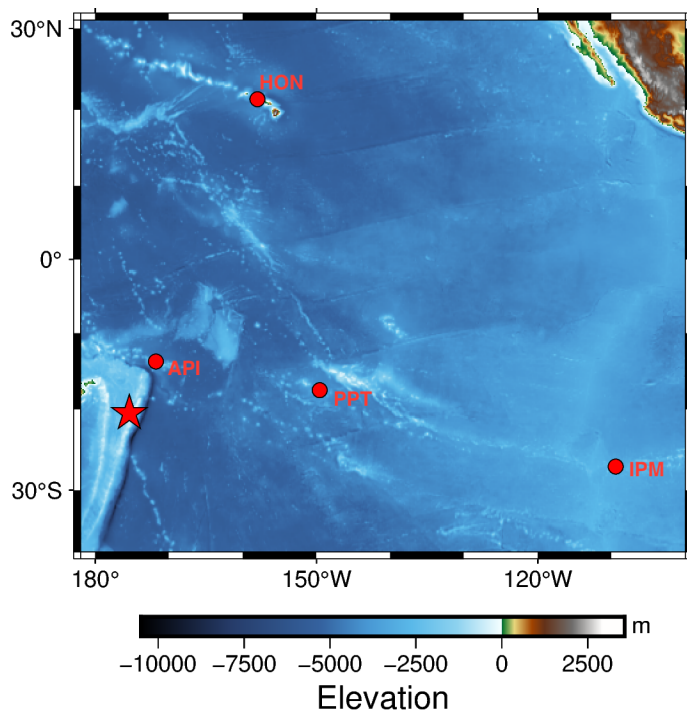


Figure S8. Map of the mid-Pacific observatories.

Raw data at Japanese observatories

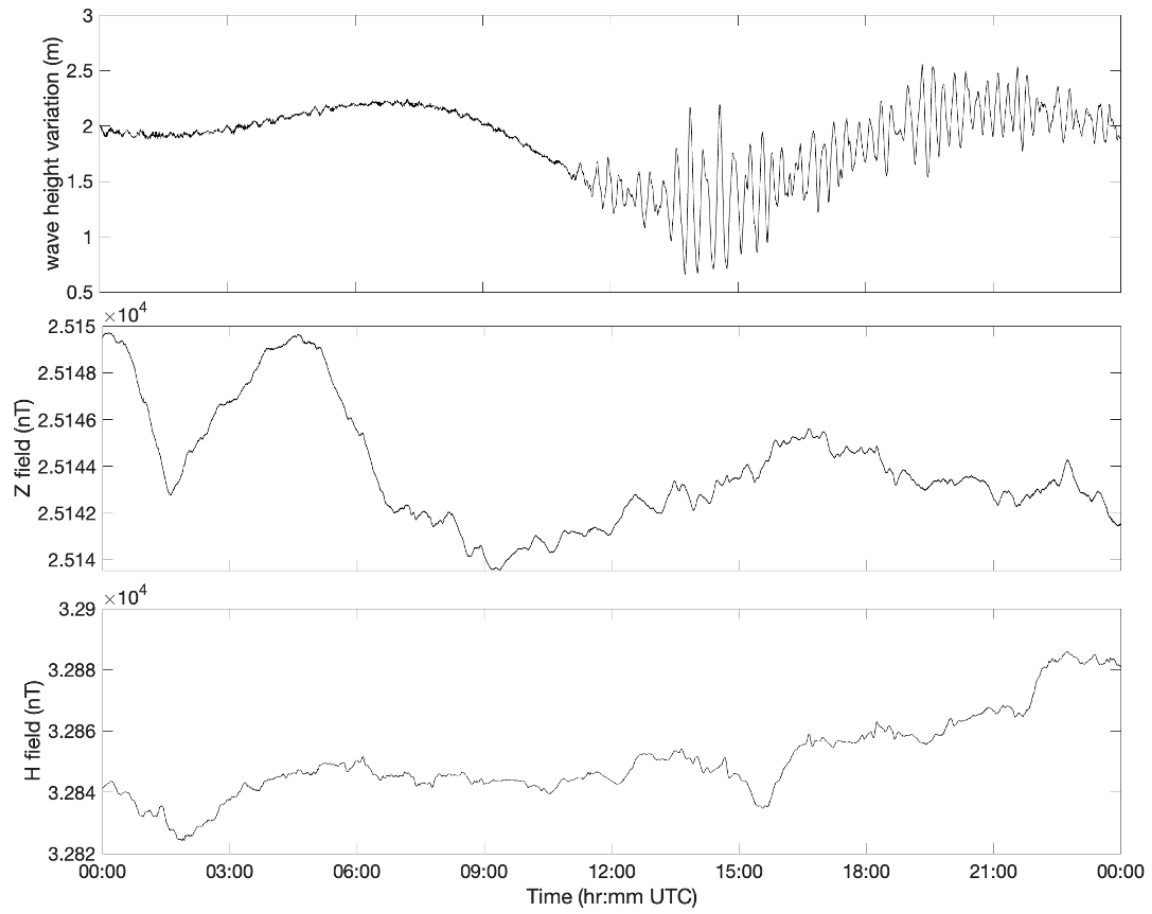


Figure S9. Raw water level variation and magnetic field data at Chichijimi Island (CBI).

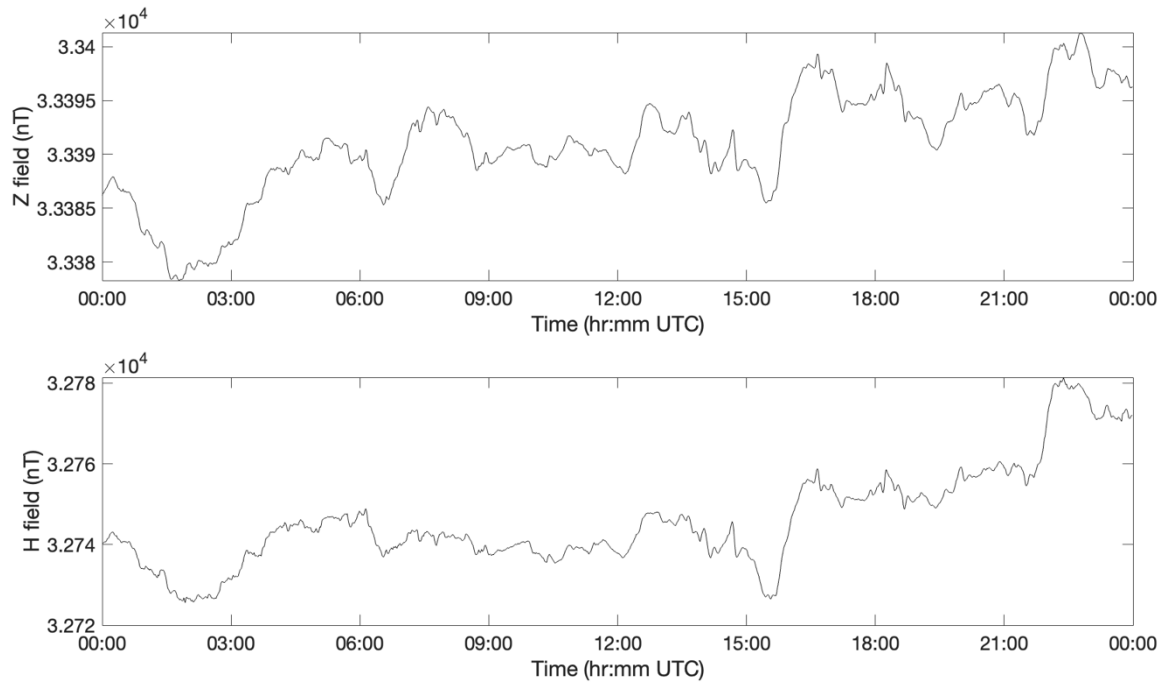


Figure S10. Raw magnetic field data at Kanoya (KNY).

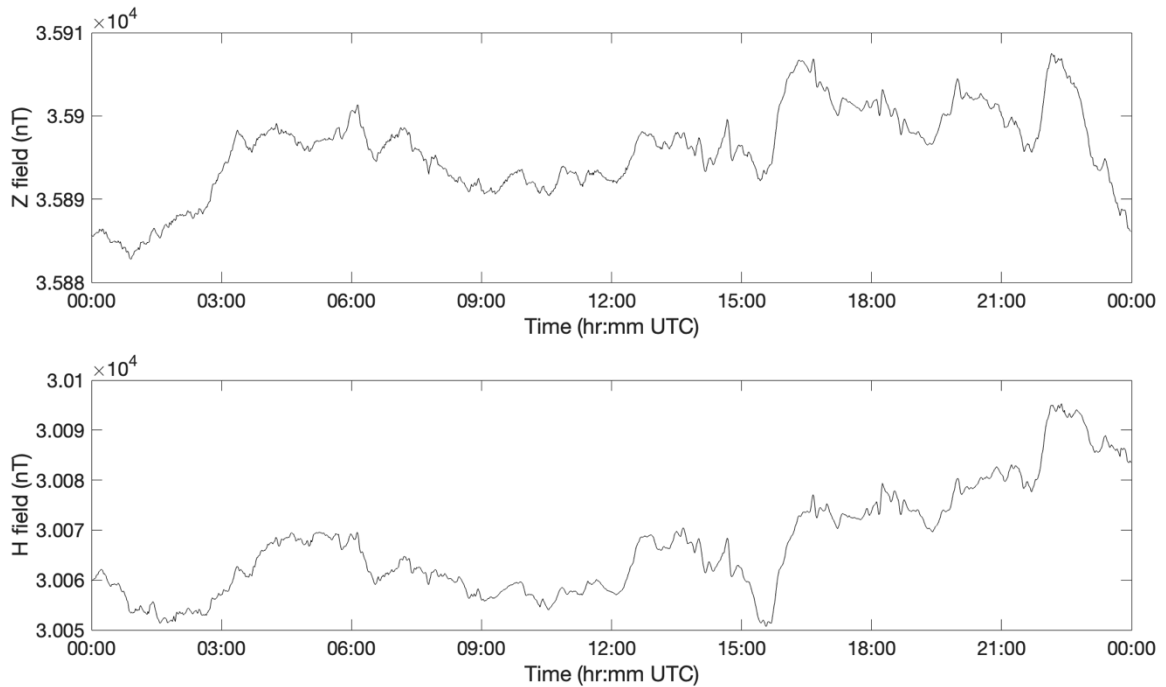


Figure S11. Raw magnetic field data at Kakioka (KAK).

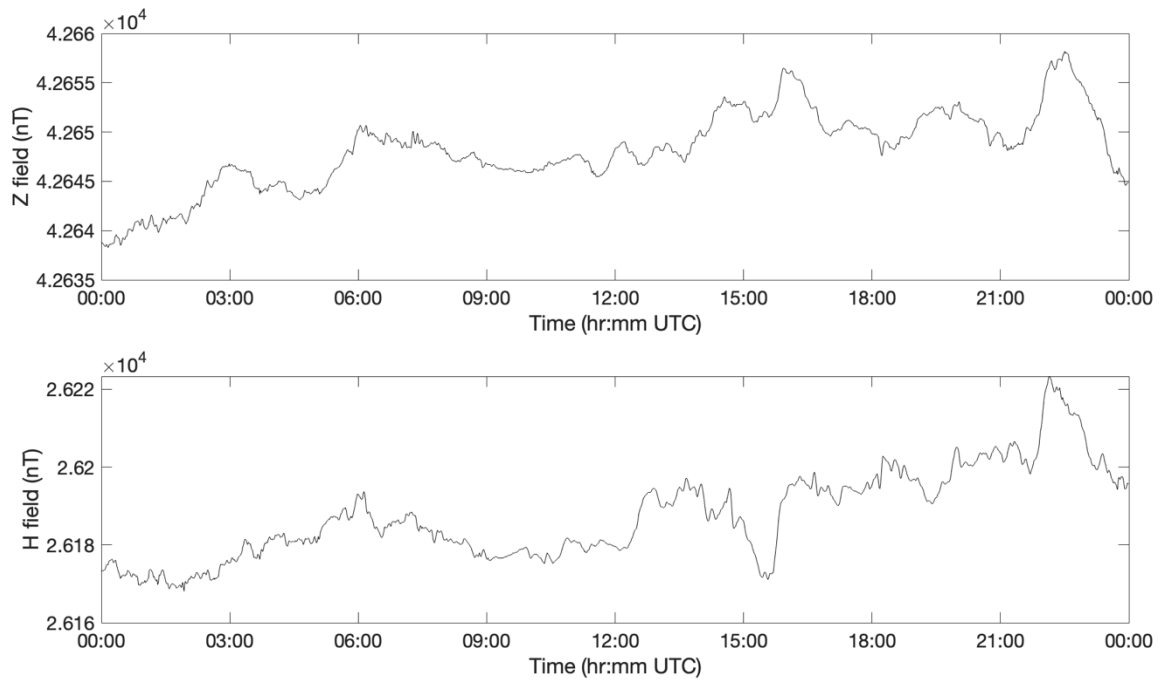


Figure S12. Raw magnetic field data at Memambetsu (MMB).

Raw data at Oceania observatories

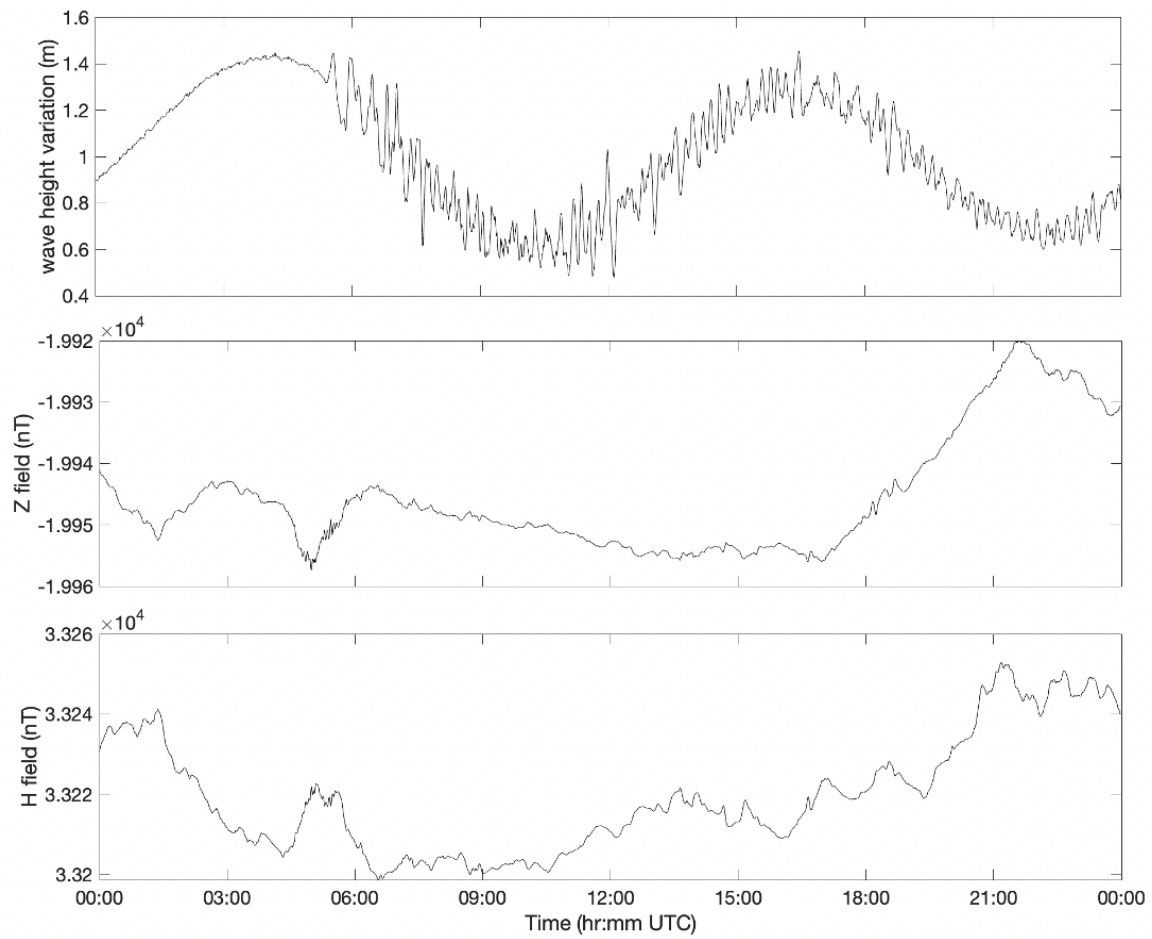


Figure S13. Raw water level variation and magnetic field data at Western Samoa (API).

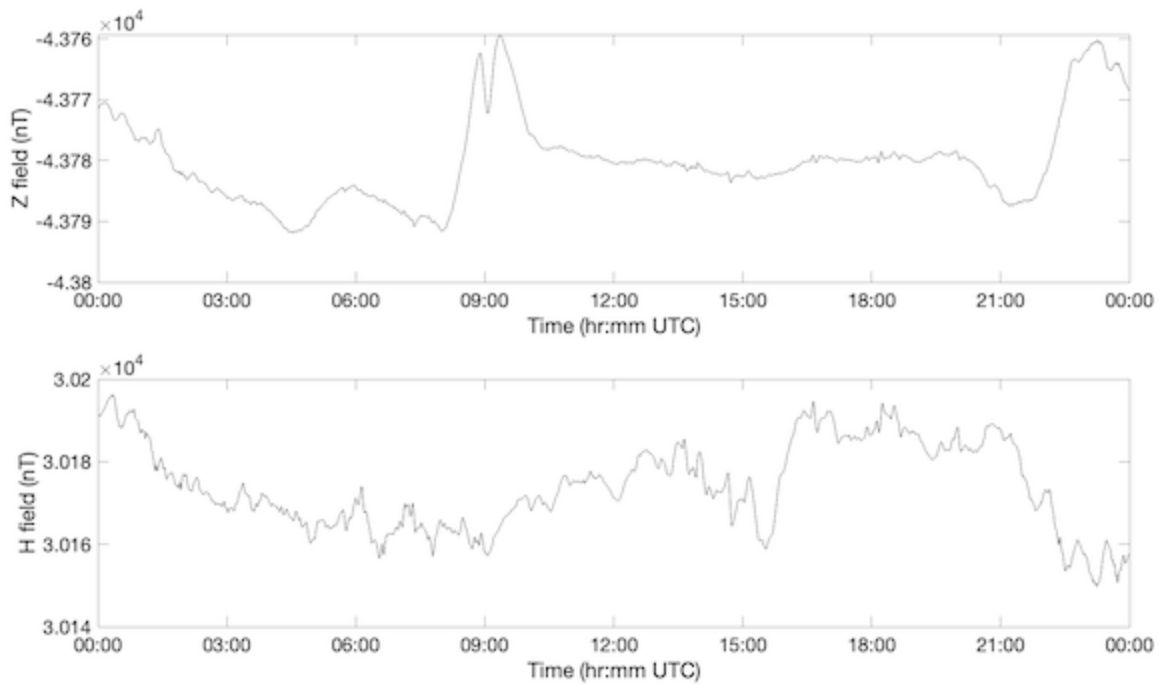


Figure S14. Raw magnetic field data at Alice Springs, Australia (ASP).

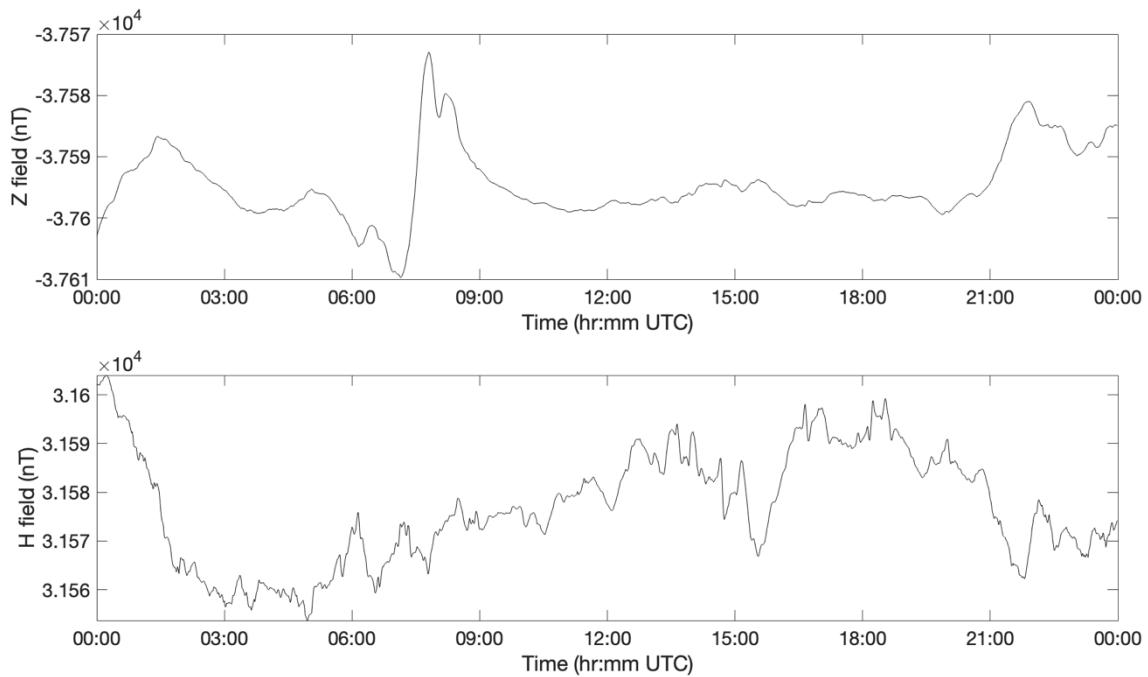


Figure S15. Raw magnetic field data at Charter Towers, Australia (CTA).

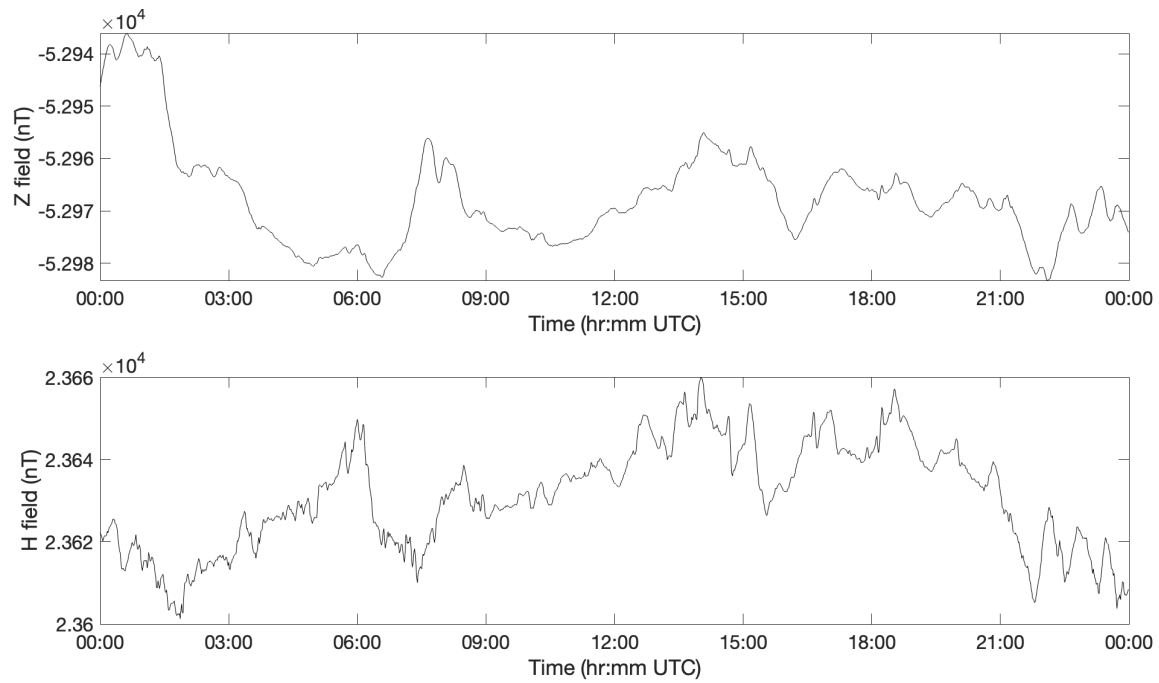


Figure S16. Raw magnetic field data at Canberra, Australia (CNB).

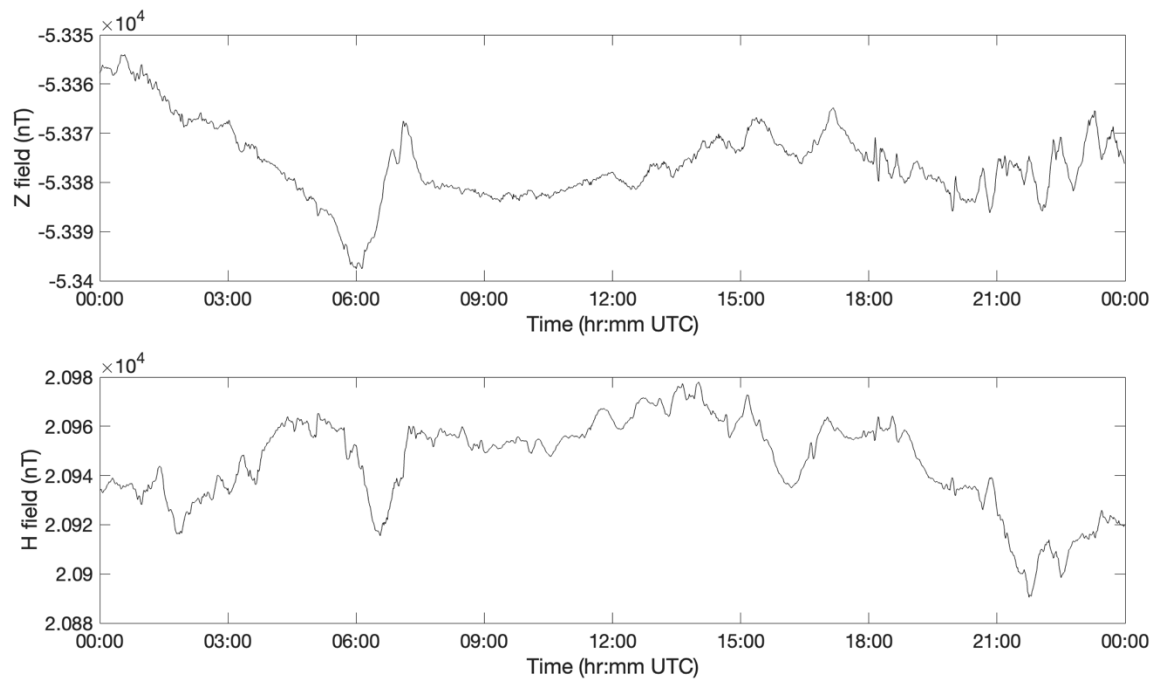


Figure S17. Raw magnetic field data at Eyrewell, New Zealand (EYR).

Raw data at mid-Pacific observatories

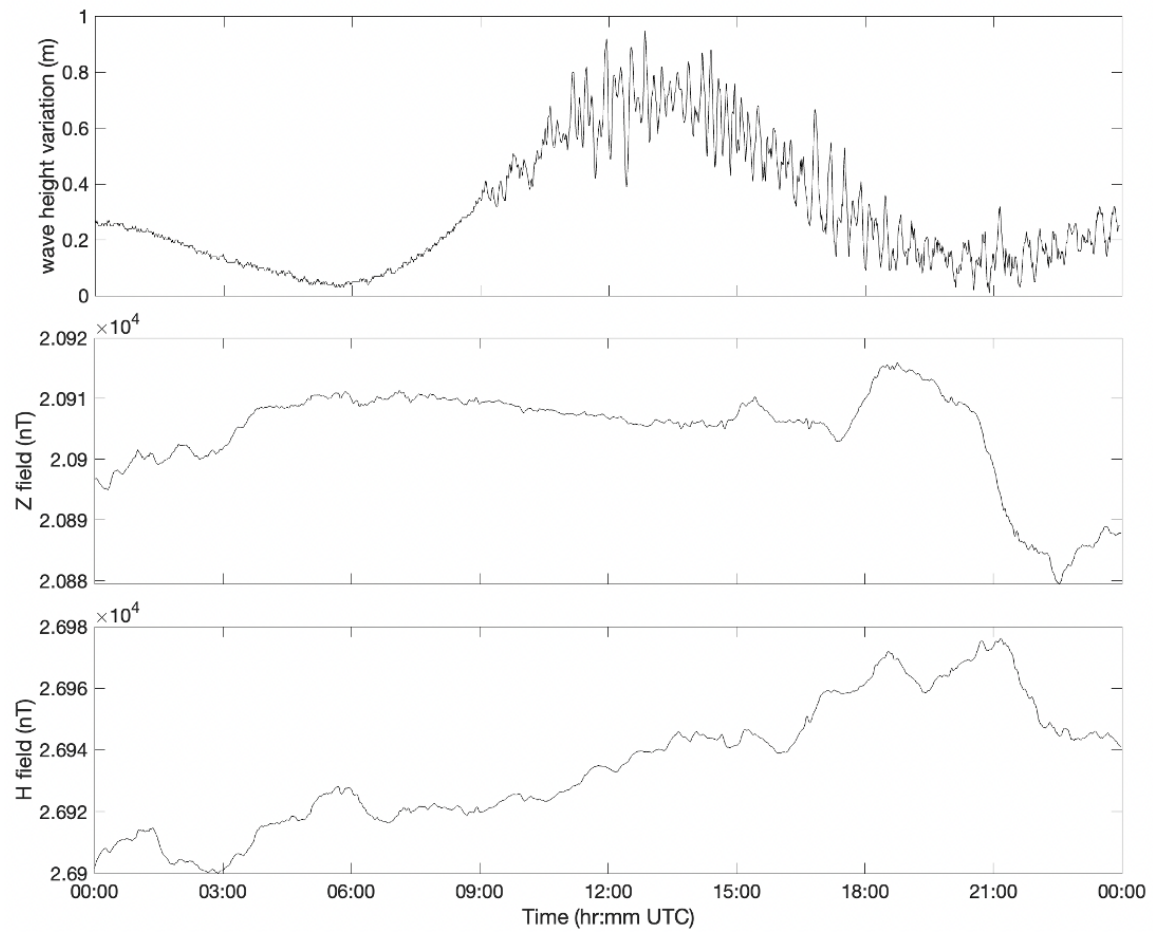


Figure S18. Raw water level variation and magnetic field data at Honolulu, USA (HON).

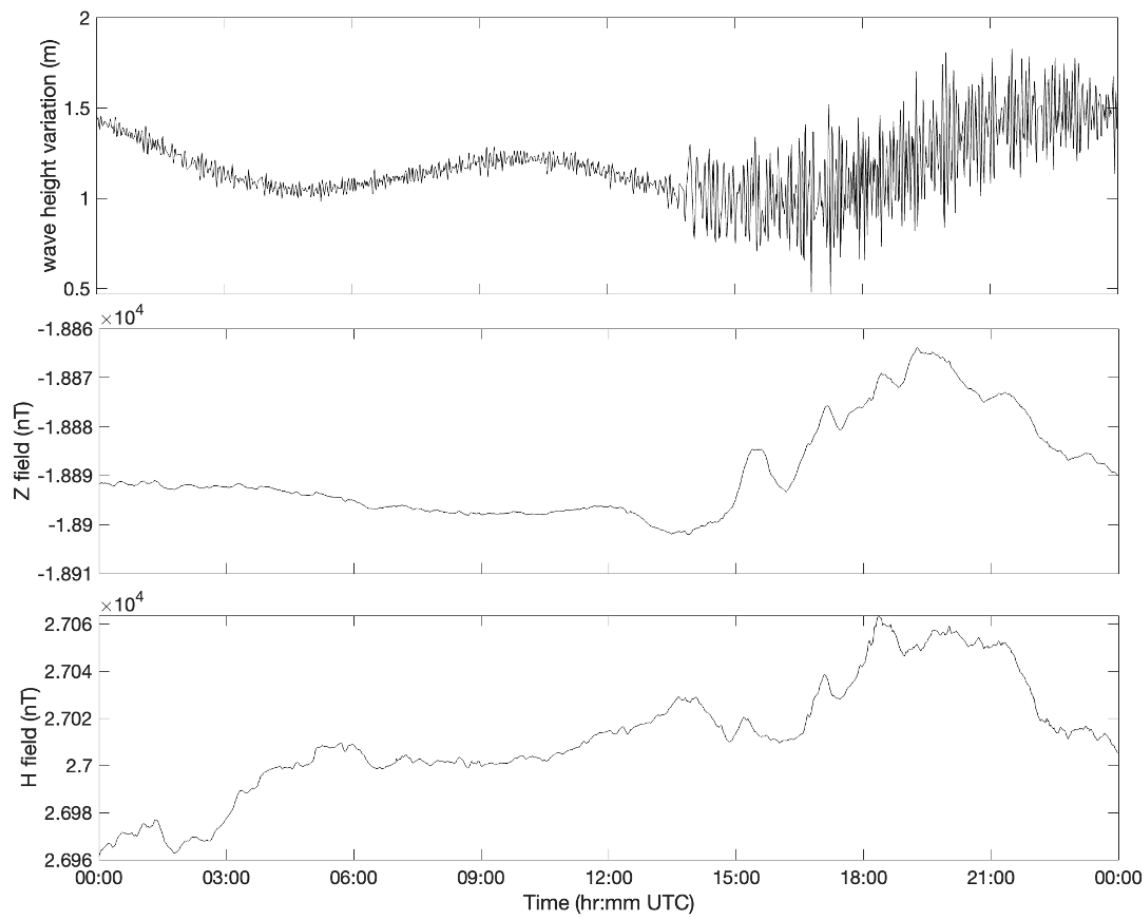


Figure S19. Raw water level variation and magnetic field data at Easter Island, Chile (IPM).

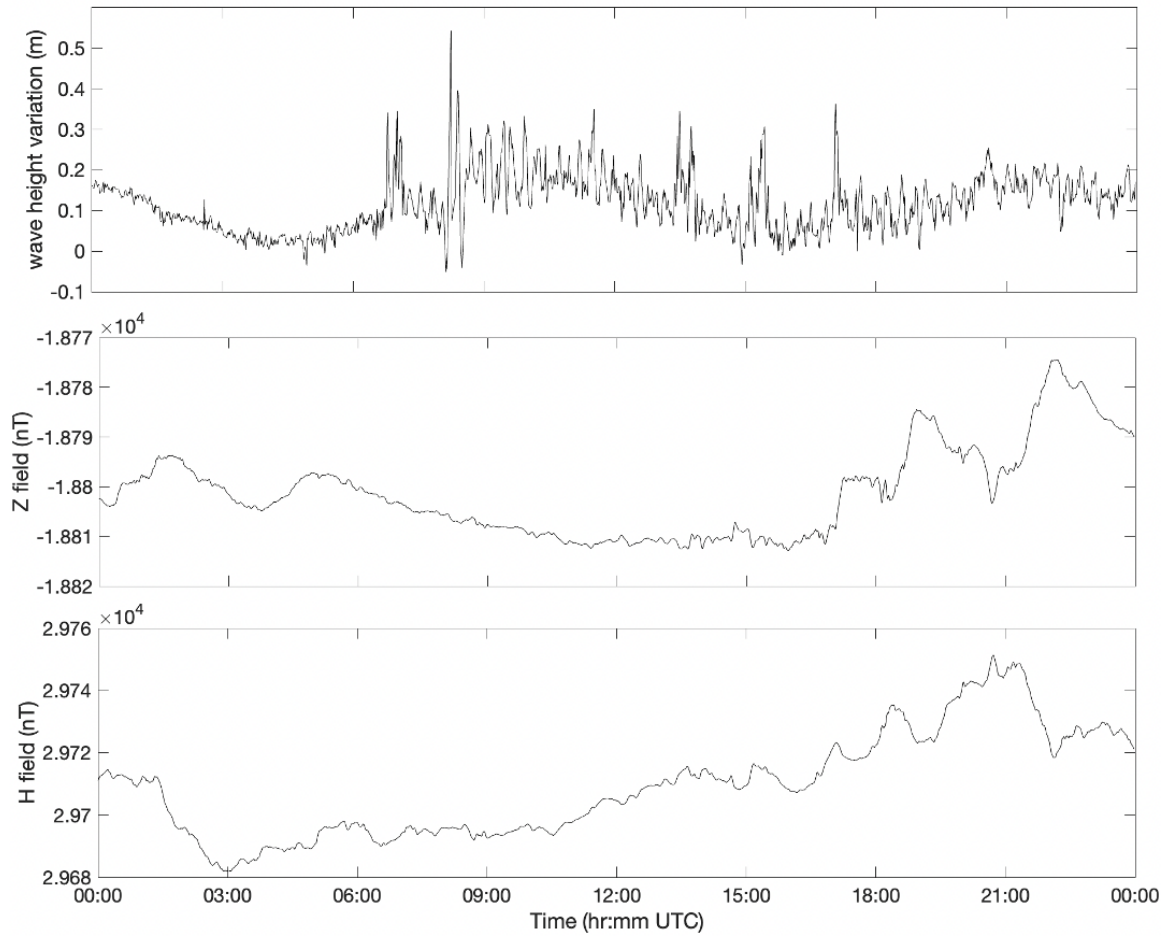


Figure S20. Raw water level variation and magnetic field data at Papeete, Tahiti, French Polynesia (PPT).

Cross-wavelet analysis spectrograms at Japanese observatories

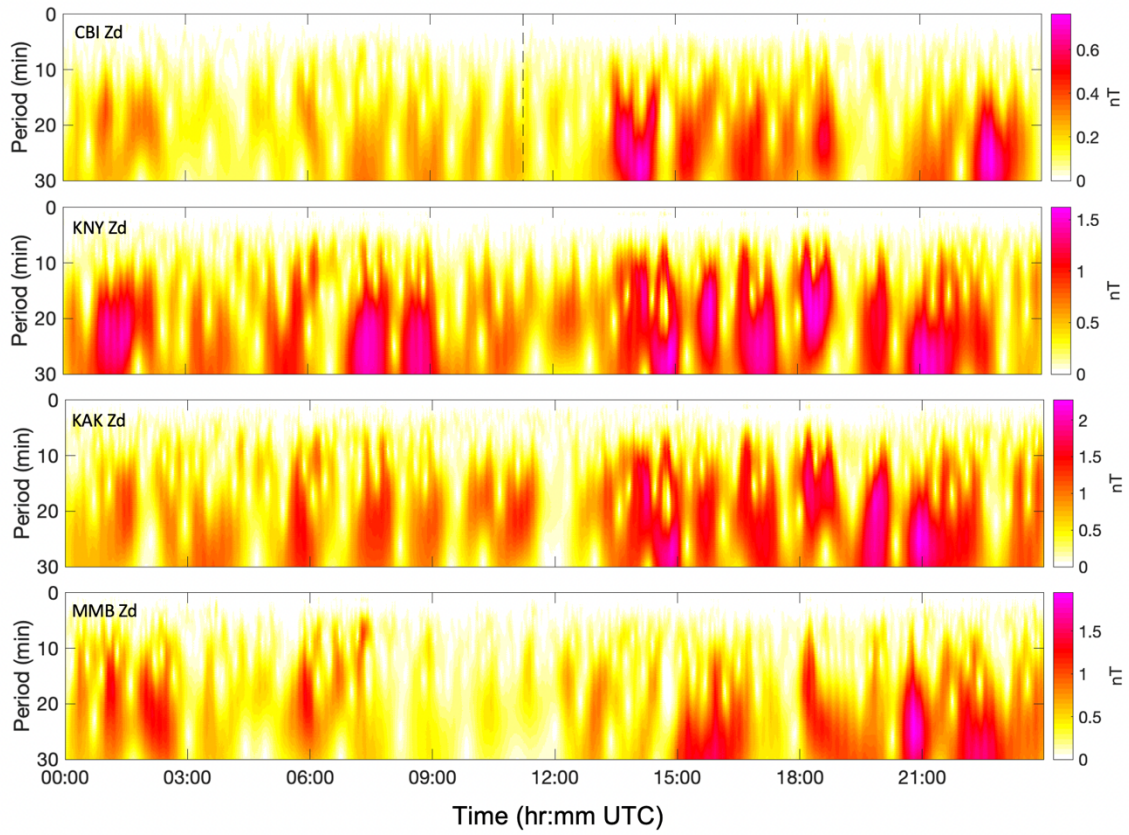


Figure S21. The cross-wavelet analysis results using $T_{\max} = 30$ minutes at the Japanese observatories.

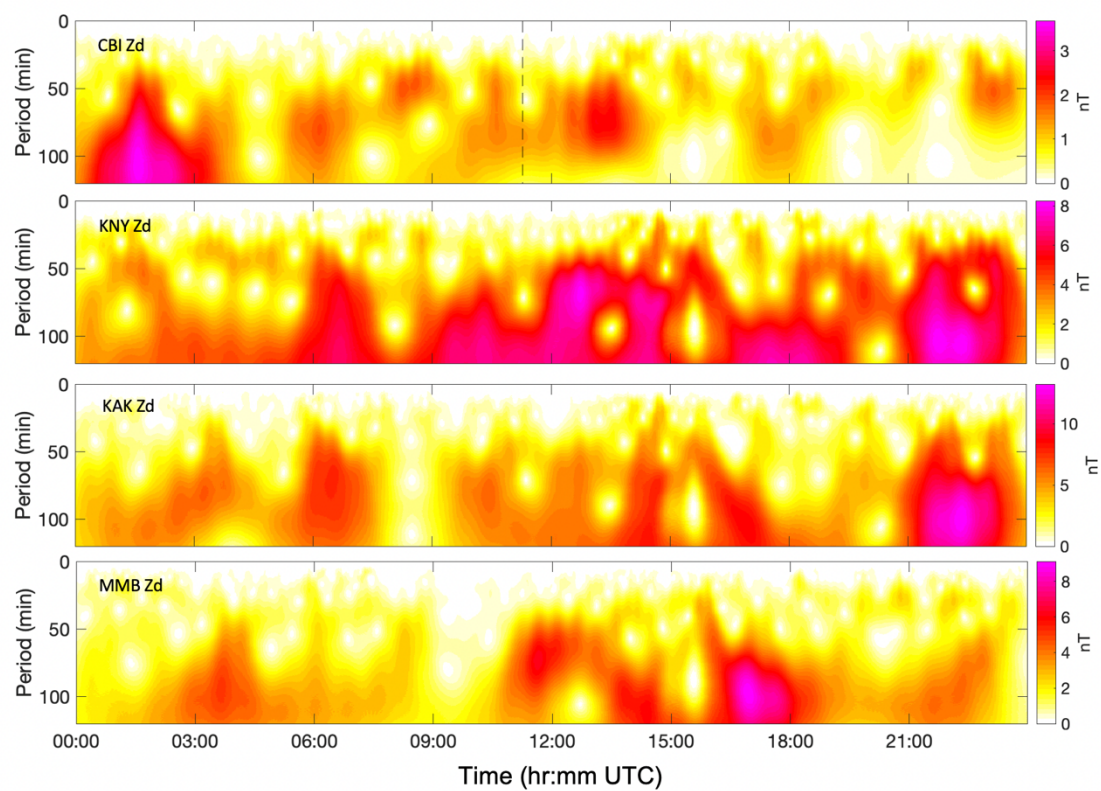


Figure S22. The cross-wavelet analysis results using $T_{\max} = 120$ minutes the Japanese observatories.

Cross-wavelet analysis spectrograms at Oceania observatories

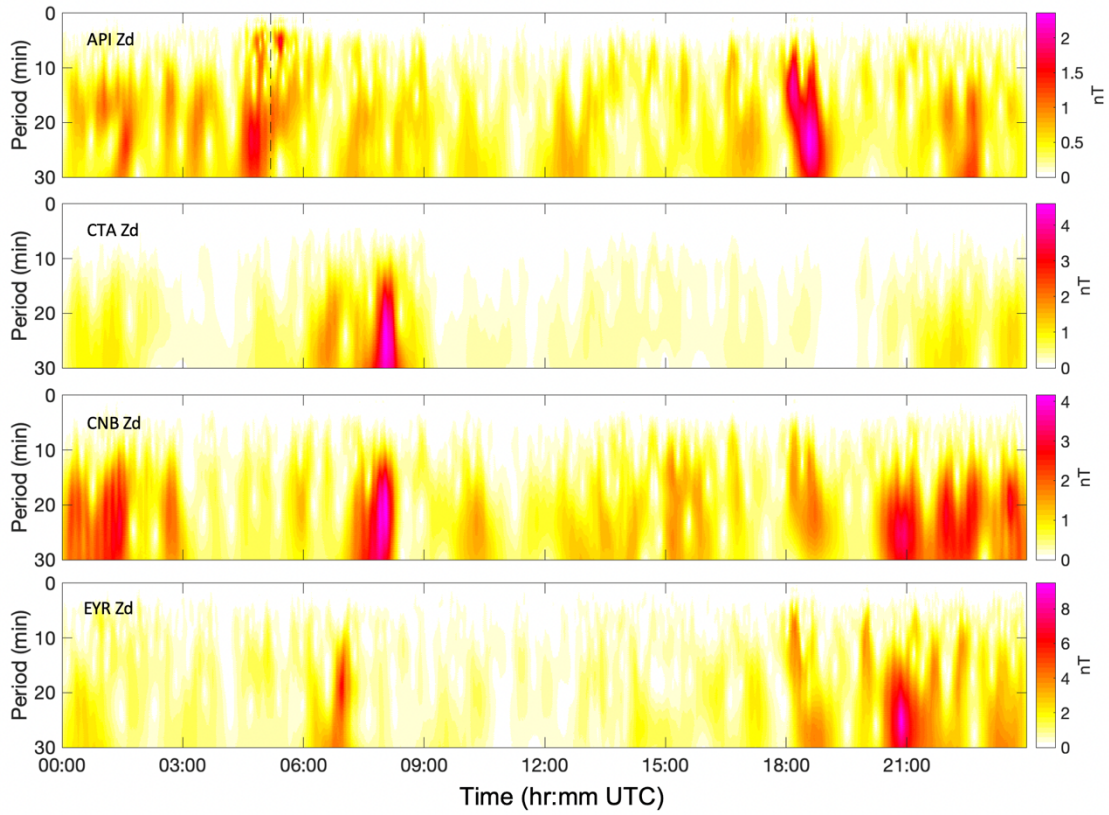


Figure S23. The cross-wavelet analysis results using $T_{\max} = 30$ minutes the Oceania observatories. The vertical dashed line denotes the Western Samoa (API) water wave arrival determined from the water level data.

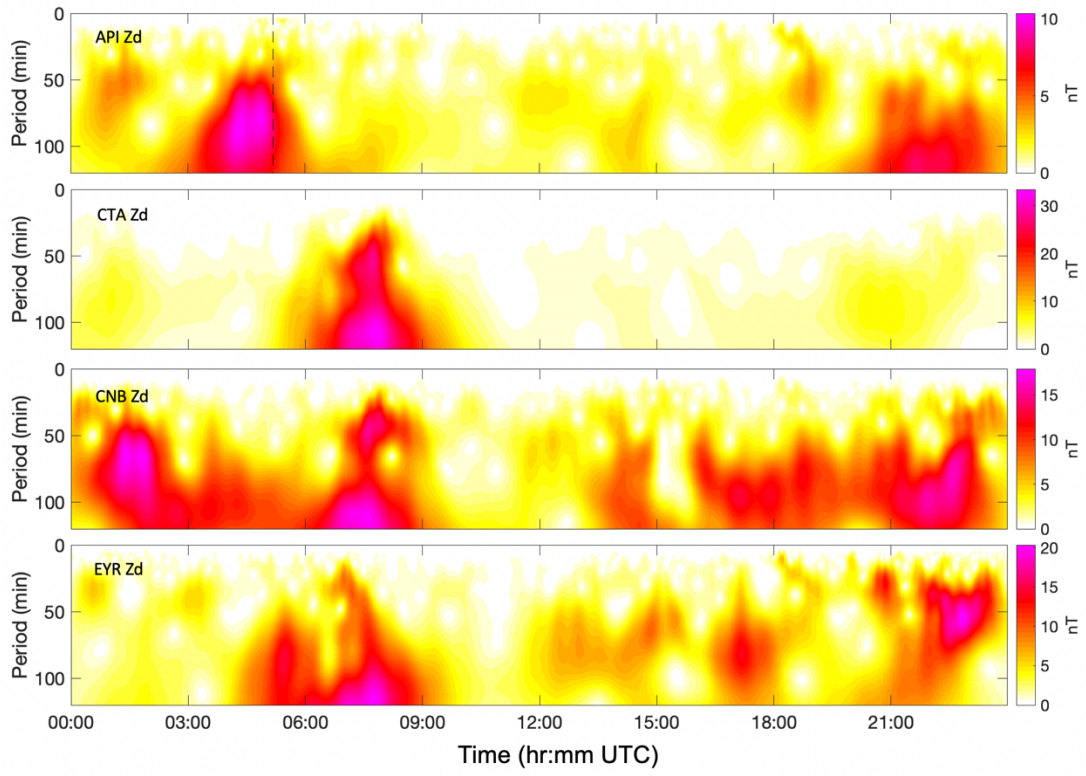


Figure S24. The cross-wavelet analysis results using $T_{\max}=120$ minutes the Oceania observatories. The vertical dashed line denotes the Western Samoa (API) water wave arrival determined from the water level data.

Cross-wavelet analysis spectrograms at mid-Pacific observatories

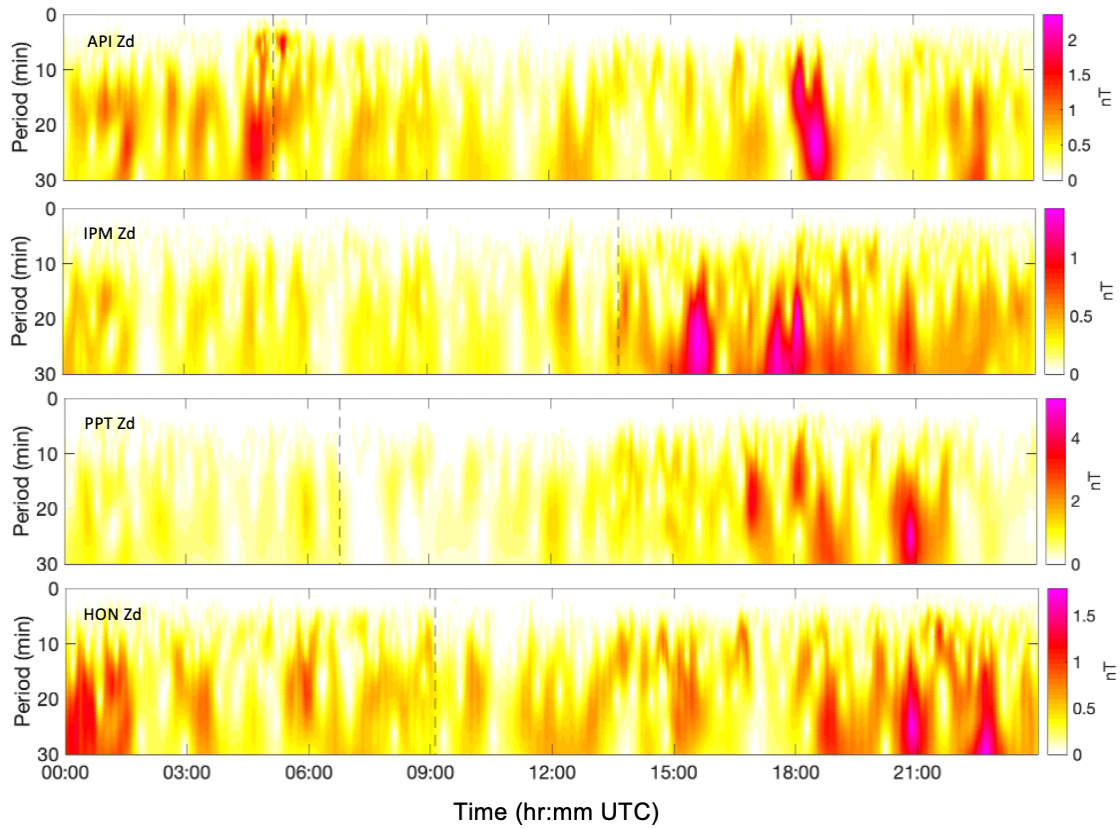


Figure S25. The cross-wavelet analysis results using $T_{\max} = 30$ minutes the mid-Pacific observatories. The vertical dashed line denotes the water wave arrival determined from the water level data.

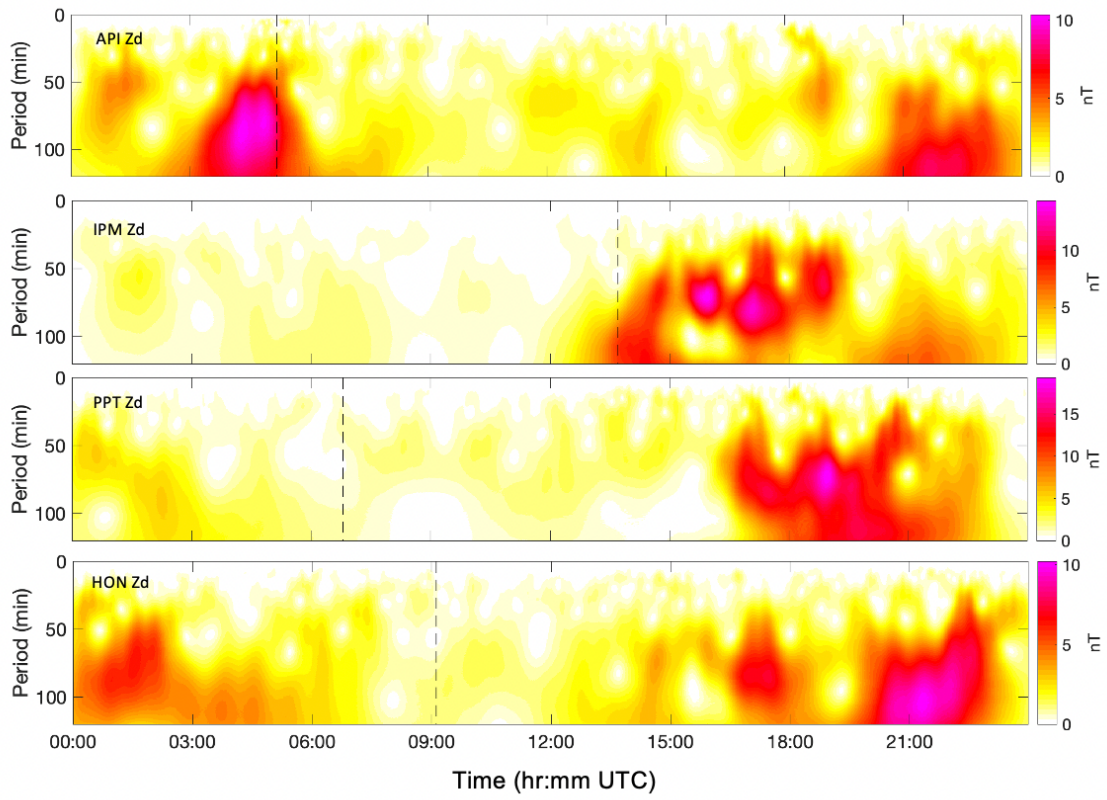


Figure S26. The cross-wavelet analysis results using $T_{\max} = 120$ minutes the mid-Pacific observatories. The vertical dashed line denotes the water wave arrival determined from the water level data.